Journal Pre-proof

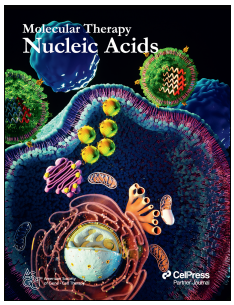

Extracellular vesicle transfer of lncRNA H19 splice variants to cardiac cells

Andreia Vilaça, Carlos Jesus, Miguel Lino, Danika Hayman, Costanza Emanueli, Cesare M. Terracciano, Hugo Fernandes, Leon J. de Windt, Lino Ferreira

PII: S2162-2531(24)00120-3

DOI: https://doi.org/10.1016/j.omtn.2024.102233

Reference: OMTN 102233

To appear in: *Molecular Therapy: Nucleic Acid*

Received Date: 1 November 2023

Accepted Date: 29 May 2024

Please cite this article as: Vilaça A, Jesus C, Lino M, Hayman D, Emanueli C, Terracciano CM, Fernandes H, de Windt LJ, Ferreira L, Extracellular vesicle transfer of lncRNA H19 splice variants to cardiac cells, *Molecular Therapy: Nucleic Acid* (2024), doi: https://doi.org/10.1016/j.omtn.2024.102233.

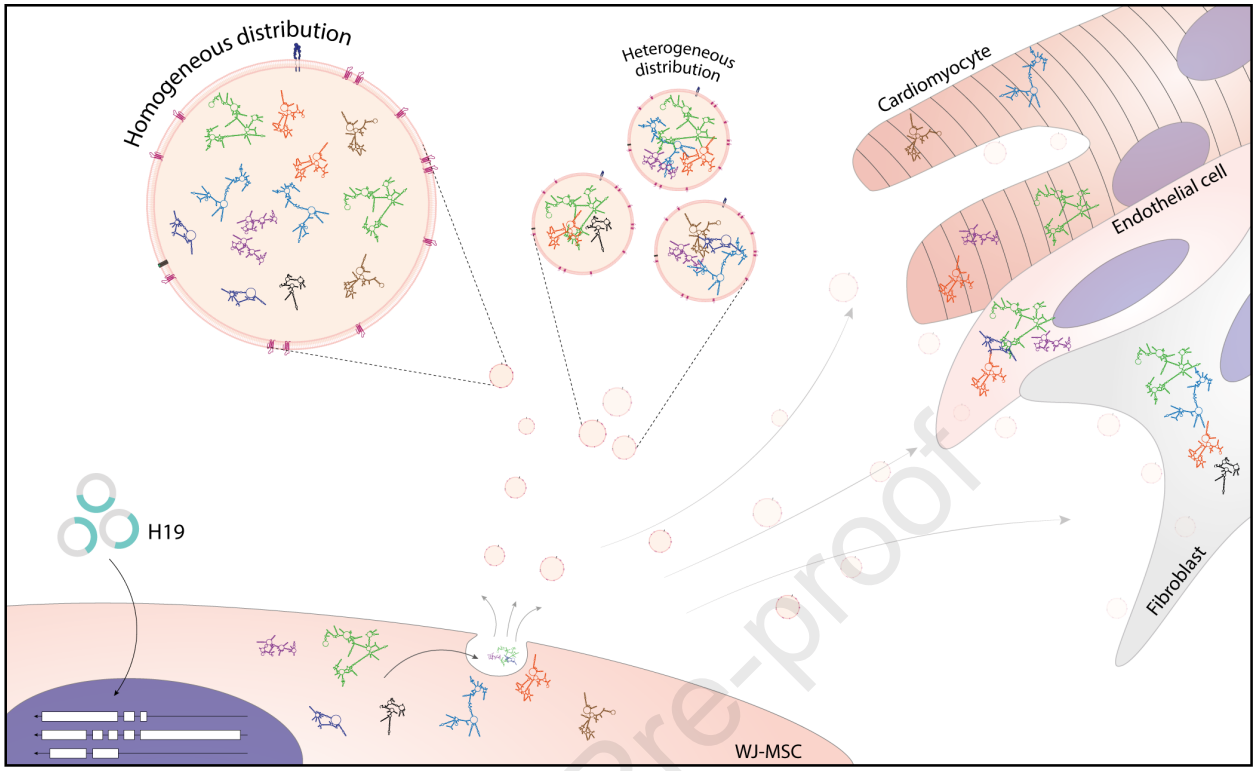

Extracellular vesicle transfer of lncRNA H19 splice variants to cardiac cells

Andreia Vilaça[1,2,4,5]; Carlos Jesus[1,3;] Miguel Lino[1,2,3]; Danika Hayman[6], Costanza Emanueli[6], Cesare M Terracciano[6], Hugo Fernandes[1,3,7*]; Leon J. de Windt[4*] and Lino Ferreira[1,3*]

[1] CNC - Center for Neuroscience and Cell Biology, CIBB - Centre for Innovative Biomedicine and Biotechnology, University of Coimbra, Coimbra, Portugal

[2] IIIUC - Institute of Interdisciplinary Research, University of Coimbra, Coimbra, Portugal

[3] FMUC - Faculty of Medicine, University of Coimbra, Coimbra, Portugal

[4] Department of Cardiology, Faculty of Health, Medicine and Life Sciences, Maastricht University, Maastricht, The Netherlands;

[5] PhD Programme in Experimental Biology and Biomedicine, Institute for Interdisciplinary Research (IIIUC), University of Coimbra, Coimbra, Portugal

[6]Imperial College London, National Heart and Lung Institute, London, United Kingdom

[7]Multidisciplinary Institute of Ageing (MIA-Portugal), University of Coimbra, Coimbra, Portugal

* These authors contributed equally

ABSTRACT

The delivery of therapeutic long non-coding RNAs (lncRNA) to the heart by extracellular vesicles (EVs) is promising for heart repair. H19, a lncRNA acting as a major regulator of gene expression within the cardiovascular system, is alternatively spliced but the loading of its different splice variants into EVs and their subsequent uptake by recipient cardiac cells remains elusive. Here, we dissected the cellular expression of H19 splice variants and their loading into EVs secreted by Wharton-Jelly mesenchymal stromal/stem cells (WJ-MSC). We demonstrated that overexpression of the mouse H19 gene in WJ-MSCs induces the expression H19 splice variants at different levels. Interestingly, EVs isolated from the H19-transfected WJ-MSC (EV-H19) showed similar expression levels for all the tested splice variant sets. In vitro, we further demonstrated that EV-H19 were taken up by cardiomyocytes, fibroblasts and endothelial cells (EC). Finally, analysis of EV tropism in rat living myocardial slices indicated that EVs were internalized mostly by cardiomyocytes and ECs. Collectively, our results indicated that EVs can be loaded with different lncRNA splice variants and successfully internalized by cardiac cells.

INTRODUCTION

Extracellular vesicles (EVs) are a class of small cell-secreted particles (30 – 1000 nm) that mediate cell-to-cell communication, by transferring RNAs and proteins incorporated during their biogenesis to target cells, ultimately modulating their function.[1, 2] In vivo data in rodent and swine models indicates that stem cell-derived EVs can be used to restrain the post-MI adverse cardiac remodeling and loss of cardiac function by promoting the survival of cardiac cells and angiogenesis.[3-6] The noncoding RNA cargo of EVs is considered to play a substantial role in the EV bioactivity.[3, 7, 8] O'Brien *et al.*, recently showed that long-noncoding RNAs (lncRNAs) can be transferred to recipient cells via EVs.[9] LncRNAs constitute a highly diverse group of transcripts, generally characterized as RNAs longer than 200 nt that do not encode functional proteins.[10] Their biogenesis, which has been shown to be distinct from that of mRNAs[11], has been linked to their specific subcellular location and function.[10] Similarly to protein-encoding genes, through alternative splicing (AS), lncRNA genes can generate several splice variants with distinct tertiary structures, new open reading frames (ORFs) for small peptides or the ability to produce different circular RNAs (circRNAs)[12] giving rise to transcripts with diverse functions.[13, 14] Since lncRNAs have important regulatory roles, the altered expression of specific splice variants should be taken into account when designing therapeutic interventions.[15]

LncRNA H19, described for the first time as a non-protein-coding RNA molecule in 1990[16], is one of the most studied lncRNAs in the cardiovascular arena. Importantly, EVs enriched in H19 have been used as a potential therapeutic platform to regenerate the heart after myocardial infarction.[17] Unfortunately, it is relatively unknown (i) which H19 splice variants are encapsulated in EVs, (ii) which H19 splice variants are delivered by EVs in different cardiac cells and (iii) what is the tropism of EVs-enriched H19 for cardiac cells. The current report attempts to address these questions.

RESULTS

To understand the impact of H19 splice variants in the cardiac context, we first analyzed the mouse H19 locus (located on chromosome 7 in the reverse strand) and identified the 16 annotated splice variants (GRCm39:CM001000.3) (**Fig. 1a**). We then designed primers to amplify different sets of H19-splice variants (**Fig. 1b**). H19 is considered conserved among humans and rodents[20]. It has been widely described that H19 expression in the mouse heart steeply diminishes throughout life[20], however, the influence of each splice variant has not been addressed before. Our results showed that, compared to the embryonic heart, the expression of all the tested splice variants was lower in 8-week adult mice hearts (**Fig. 1c**) though the decrease observed differed among the different sets of splice variants. The higher downregulation through development was seen for Set B and C. Set D and E were decreased to a lower extent in the adult mouse heart while Set A suffers the least downregulation. Overall, regardless of the splice variant set, H19 expression decreased during development which might, at least partially, explain the decreased regenerative capacity of the adult heart.

Due to its large size[21], it is not feasible to chemically synthetize H19 and therefore earlier studies have mostly relied on the use of viral vectors to overexpress H19 in target cells. Herein, we analyzed the expression of H19 splice variants following the overexpression of H19 in WJ-MSCs and their subsequent sorting into EVs. MSCs were used as EV donors due to their desirable immunomodulatory properties and the cardiac protective and pro-regenerative effects of the secreted EVs.[22, 23] Human WJ-MSC were transfected with mammalian expression vectors and harvested after 48 h (**Fig. 2a**). RT-qPCR analysis of splice variant sets expression demonstrated that H19 transfection significantly increased the expression of all tested H19 splice variants sets on average ~230 to 6176 copies/ng RNA (**Fig. 2b**). Then, EVs secreted from mock or H19 transfected cells, hereafter referred to as EV-Entry or EV-H19, were isolated from the conditioned medium. EV characterization demonstrated that EV-Entry and EV-H19

had similar sizes (**Fig. 2c**), concentration yield (**Fig. 2d**), zeta potential (**Fig. 2e**), protein concentration (**Fig. 2f**) and purity (**Fig. 2g**). Western blot characterization of EV lysates confirmed expression of CD9 and CD63 as well as GAPDH and absence of calnexin consistent with a small EV preparation from cell culture origin (**Fig. S1**).

Splice variants may be differentially sorted into EVs at the parental cell due to specific interactions of the transcript with RNA binding proteins involved in the RNA export to EVs. To assess the presence of H19 splice variants in EVs, RT-qPCR analysis was performed on EV-Entry and EV-H19 (**Fig. 2h**). Our results showed that all evaluated splice variant sets were present in the EVs at higher copy number (**Fig. 2h**) per ng of RNA compared to their expression by the parental cells (**Fig. 2b**). Expression of Set B and C in EV-H19 was increased to similar levels. Notably, Set A and D, which showed low expression in H19-transfected WJ-MSC, were shown to be expressed at higher levels in EVs, comparable to Set B and Set C which were highly expressed in the WJ-MSC after transfection. Strikingly, Set E, which showed a low expression in H19 transfected WJ-MSC, was detected in the EV-H19 (mean of ≈12.000 copies/ng of total RNA) albeit with a lower expression compared to the other splice variant sets.

The distribution of the splice variants among the individual EVs in the sample remains elusive and it is still unclear if all the isoforms are present within a single EV or if different isoforms are loaded in specific EV subpopulations. Understanding the uptake of EVs by the recipient cells and their capacity to transfer RNAs may provide further insights on the distribution of the different splice variants in the EV sample. To evaluate EV uptake by the major cardiac cell types, we treated neonatal mouse cardiomyocytes (**Fig. 3a**), mouse neonatal cardiac fibroblasts (**Fig. 3c**) and mouse aortic endothelial cells (MAECs) (**Fig. 3e**) with 3×10^{10} part/mL WJ-MSC PKH67-labelled EVs for 4 h. Confocal imaging suggested that EVs were internalized by all the cardiac cell types evaluated. Moreover, our results showed that

fibroblasts internalized higher levels of EVs (87.6% ± 11.2) than cardiomyocytes (51.2% ± 8.3) and MAECs (59.8% ± 22.3) (**Fig. S2**). Interestingly, neonatal mouse cardiomyocytes showed a larger EV foci size when compared to both cardiac fibroblasts and MAECs (**Fig. 3; Fig. S2c)**. We further compared the EV internalization level of adult mouse cardiomyocytes (16.6% ± 16.1) which was found to be lower and more variable than in neonatal mouse cardiomyocytes (**Fig. S2d-f**).

Next, to evaluate RNA transfer from the EVs to the recipient cells, we treated neonatal mouse cardiomyocytes (**Fig. 3b**), mouse neonatal cardiac fibroblasts (**Fig. 3d**) and MAECs (**Fig. 3f**) with EV-Entry or EV-H19 for 4 h and assessed the H19 splice variant copy number by RT-qPCR. Preliminary results obtained by us indicate that H19 transcripts transported within the EVs were functional upon delivery to the recipient cells (**Fig. S3**). Cardiomyocytes (**Fig. 3b**) were shown to express very low levels of Set A, B and D and higher expression of Set C. Set E was not detected in cardiomyocytes. Upon treatment with EV-H19, there was a significant increase in the expression of Set A, B and D, demonstrating the transfer of RNA from the EVs to cardiomyocytes within 4 h. An increase in Set E was also detected in EV-H19 treated cardiomyocytes, although not statistically significant. Interestingly, expression of Set C that were already highly expressed in cardiomyocytes, was not affected by EV-H19 uptake. Fibroblasts (**Fig. 3d**) showed a low expression of Set B and D and higher expression of Set C. Contrarily, Set A and E were not detected in fibroblasts. Treatment with EV-H19 induced a statistically significant increase in the expression of Set A, B and D. Expression of Set E and C was also increased by EV-H19 treatment although the difference was not statistically significant. ECs (**Fig. 3f**) express very low amounts of Set A, B and D whereas the expression of Set C was slightly higher. Similar to cardiomyocytes and fibroblasts, Set E expression was undetected in ECs. Treating ECs with EV-H19 for 4 h induced a statistically significant increase in the expression of Set B and D and, although not significant, an increase in the

expression of Set A and C was also observed. Intriguingly, Set E expression was not altered by EV-H19 uptake remaining undetected after EV-H19 treatment. Notably, compared to cardiomyocytes and fibroblasts, the limited increase in the expression of the H19 splice variants in ECs is in line with the lower internalization profile observed with native EV labelled with PKH67 (**Fig. 3e**). Lastly, we compared the expression of EV-H19 from WJ-MSC with direct transfection of the H19 plasmid in ECs (recipient cells). Our results show higher expression of the splice variants in EV-H19 than in cells transfected with H19 plasmid (**Fig. 2h vs Fig. S4**)

EV uptake in different cardiac cell types has been demonstrated in vitro but uptake in more complex models has not been fully explored. To understand the natural tropism of EVs in a more complex cardiac setting whilst avoiding the influence of systemic interactions, we made use of cardiac slices.[24] The organotypic heart slice preparations are thin (< 400 µm) enough to ensure sufficient oxygen supply and diffusion of metabolic waste while retaining the native cellular composition, architecture and physiology of the heart *in vitro.* Hypoxia-reoxygenation was induced in these organotypic cultures (see Materials and Methods section) before exposure to EVs. Rat cardiac slices were treated with 1 x 10^8 native WJ-MSC PKH67-labelled EVs for 24 h. Confocal imaging analysis of the number of EV *foci* colocalizing with cardiomyocytes ($PKH67^+$/cardiac troponin T^+) or ECs ($PKH67^+$/ isolectin $B4^+$) demonstrated that the majority of EVs were taken up and processed, both by cardiomyocytes and ECs but also other cell types (**Fig. 4a, 4b**) (CM: 32.50 ± 24.48; EC: 33.17 ± 48.08; other: 5.17 ± 5.50; values represent the sum of *EV foci* per cell type in all images acquired for one cardiac slice sample). Of notice, analysis of EV distribution (**Fig. S5**) in "z" within the cardiac slice 24 h post treatment showed that the PKH67 signal was observed not only at the surface but also in deeper cell layers both for cardiomyocytes and ECs. Since cardiomyocytes and ECs were not presented in similar proportions in the slices, accurate analysis of tropism might require information on the cellular composition of the rat heart. Although it is commonly accepted that

cardiomyocytes represent 30% of the heart cells[25], initial studies of the rat heart have shown that cardiomyocytes account for around 75% of the volume of the heart while ECs only take up 3% of the volume.[26] Here we hypothesize that higher surface-area-to-volume ratio of the cardiomyocytes would provide increased opportunity for interaction and internalization of EVs similarly to what was seen for nanoparticles[27], rather than specific tropism to cardiomyocytes. Remarkably, the EV *foci* quantified within cardiomyocytes and ECs was similar and each represented around 50% of the total quantified EV *foci* suggesting a preferential uptake by ECs since they are expected to only represent 3% of the volume of the heart. However, it is important to note that a single cardiomyocyte could span more than one "Z". This is difficult to account for in the analysis due to multinucleation of cardiomyocytes which impedes accurate distinction and quantification of a single cardiomyocyte.

DISCUSSION

Here, we provide evidence that EVs can be loaded with different H19 splice variants and successfully delivered to different cardiac cell types both in 2D cultures as well as in more physiologically relevant models (ex-vivo cardiac slices). Our results suggest that upon transcription of H19 splice variants in the EV-secreting cells, the different variants were sorted to EVs. Currently, literature on the mechanisms governing lncRNA packaging and sorting to EVs are scarce. The protein heterogeneous nuclear ribonucleoprotein A2B1 (hnRNPA2B1) has been the only one already described to bind to[28] and mediate H19 packaging and sorting to EVs[29], although the exact mechanism has not been dissected.

Our *in vitro* results further show that fibroblasts higher internalized EVs than cardiomyocytes and MAECs. The larger EV foci size in cardiomyocytes than in other cardiac cells suggest higher intracellular accumulation of EVs, likely in the endolysosomal compartment, but this requires further testing in the future. While our findings align with

previous research[30], other EV internalization studies have demonstrated opposite profiles, with ECs being the cell type that takes up the most EVs.[17] This is likely due to differences in the source of EVs, EV dose and treatment duration as well as inherent differences in the cell models used to test the internalization. Interestingly, our studies of EVs with cardiac slices suggest that ECs are the cardiac cells that internalize more EVs. At the moment, it is not clear the reasons for the differences obtained between isolated cells and cardiac slices; however, it shows the importance of having different cellular and *ex-vivo* models to fully investigate the interaction of EVs with tissues/organs.

Although it is not clear whether lncRNA packing into EVs is done in a homogenous (each EV contains similar amounts of a given transcript) or in a heterogenous way (transcripts are distributed differently within each EV), the differences observed in the internalization profile of each cell type hint towards the latter process being the most likely. If heterogenous distribution of the transcripts among the individual EVs would take place, that would for instance explain why Set E is not detected in ECs while it was found in EVs and then in fibroblasts.

Further research into the relevance of each splice variant in the context of cardiac disease and how to manipulate their expression in EVs could improve therapeutic potential by selectively delivering the required splice variants to the target cells.

MATERIALS and METHODS

Due to space limitations, the Materials and Methods section can be found online in the Supplementary Information file.

DATA AND CODE AVAILABILITY

Data that support the findings of this study are available from the corresponding author upon request.

SUPPLEMENTAL INFORMATION

Supplemental information can be found online.

KEYWORDS

Extracellular vesicles, RNA therapeutics, splice variants, H19 lncRNA

ACKNOWLEDGEMENTS

The authors would like to acknowledge Crioestaminal (www.crioestaminal.pt) for providing samples and other helpful information and Dr. Yingqun Huang for providing the lncRNA H19 plasmid. The authors would further like to acknowledge the funding by the FCT PhD Studentships (SFRH/BD/119187/2016 & SFRH/BD/ 144092/2019), Programa Operacional Competividade e Internacionalização (POCI) na sua componente FEDER e pelo orçamento da Fundação para a Ciência e a Tecnologia na sua componente OE (Project 2022.03308.PTDC); EC projects RESETageing (Ref. 952266) and REBORN (Ref. 101091852); and PRR project HfPT- Health from Portugal (Ref: 02/C05-i01.01/2022.PC644937233-00000047). L.D.W. acknowledges support from the Dutch CardioVascular Alliance (ARENA-PRIME). L.D.W. was further supported by a VICI award 918-156-47 from the Dutch Research Council, Marie Sklodowska-Curie grant agreement no. 813716 (TRAIN-HEART) and a PPP Allowance made available by Health~Holland, Top Sector Life Sciences & Health under agreement LSHM21068, to stimulate public-private partnerships.

AUTHOR CONTRIBUTIONS

A.V., C.J., M.L., D.H., conducted the experiments. A.V., C.J., H.F, L. W. and L.F. designed the experiments. A.V., C.J., M.L., D.H., C.E., C.T., H.F., L.W. and L.F. analyzed the experiments. A.V., C.J. analyzed the data. A.V., C.J., H.F, L.W. and L.F. wrote the paper.

DECLARATION OF INTERESTS

The authors declare no competing interests.

REFERENCES

1. Vilaca, A, de Windt, LJ, Fernandes, H, and Ferreira, L (2023). Strategies and challenges for non-viral delivery of non-coding RNAs to the heart. *Trends Mol Med* **29**: 70-91.
2. de Abreu, RC, Fernandes, H, da Costa Martins, PA, Sahoo, S, Emanueli, C, and Ferreira, L (2020). Native and bioengineered extracellular vesicles for cardiovascular therapeutics. *Nat Rev Cardiol* **17**: 685-697.
3. Agarwal, U, George, A, Bhutani, S, Ghosh-Choudhary, S, Maxwell, JT, Brown, ME, Mehta, Y, Platt, MO, Liang, Y, Sahoo, S*, et al.* (2017). Experimental, Systems, and Computational Approaches to Understanding the MicroRNA-Mediated Reparative Potential of Cardiac Progenitor Cell-Derived Exosomes From Pediatric Patients. *Circ Res* **120**: 701-712.
4. Gallet, R, Dawkins, J, Valle, J, Simsolo, E, de Couto, G, Middleton, R, Tseliou, E, Luthringer, D, Kreke, M, Smith, RR*, et al.* (2017). Exosomes secreted by cardiosphere-derived cells reduce scarring, attenuate adverse remodelling, and improve function in acute and chronic porcine myocardial infarction. *Eur Heart J* **38**: 201-211.
5. Zhu, LP, Tian, T, Wang, JY, He, JN, Chen, T, Pan, M, Xu, L, Zhang, HX, Qiu, XT, Li, CC*, et al.* (2018). Hypoxia-elicited mesenchymal stem cell-derived exosomes facilitates cardiac repair through miR-125b-mediated prevention of cell death in myocardial infarction. *Theranostics* **8**: 6163-6177.
6. Barile, L, Lionetti, V, Cervio, E, Matteucci, M, Gherghiceanu, M, Popescu, LM, Torre, T, Siclari, F, Moccetti, T, and Vassalli, G (2014). Extracellular vesicles from human cardiac progenitor cells inhibit cardiomyocyte apoptosis and improve cardiac function after myocardial infarction. *Cardiovasc Res* **103**: 530-541.
7. Cambier, L, de Couto, G, Ibrahim, A, Echavez, AK, Valle, J, Liu, W, Kreke, M, Smith, RR, Marban, L, and Marban, E (2017). Y RNA fragment in extracellular vesicles confers cardioprotection via modulation of IL-10 expression and secretion. *EMBO Mol Med* **9**: 337-352.
8. Gollmann-Tepekoylu, C, Polzl, L, Graber, M, Hirsch, J, Nagele, F, Lobenwein, D, Hess, MW, Blumer, MJ, Kirchmair, E, Zipperle, J*, et al.* (2020). miR-19a-3p containing exosomes improve function of ischaemic myocardium upon shock wave therapy. *Cardiovasc Res* **116**: 1226-1236.
9. O'Brien, K, Breyne, K, Ughetto, S, Laurent, LC, and Breakefield, XO (2020). RNA delivery by extracellular vesicles in mammalian cells and its applications. *Nat Rev Mol Cell Biol* **21**: 585-606.
10. Statello, L, Guo, CJ, Chen, LL, and Huarte, M (2021). Gene regulation by long non-coding RNAs and its biological functions. *Nat Rev Mol Cell Biol* **22**: 96-118.
11. Quinn, JJ, and Chang, HY (2016). Unique features of long non-coding RNA biogenesis and function. *Nat Rev Genet* **17**: 47-62.
12. Aznaourova, M, Schmerer, N, Schmeck, B, and Schulte, LN (2020). Disease-Causing Mutations and Rearrangements in Long Non-coding RNA Gene Loci. *Front Genet* **11**: 527484.
13. Li, X, He, X, Wang, H, Li, M, Huang, S, Chen, G, Jing, Y, Wang, S, Chen, Y, Liao, W*, et al.* (2018). Loss of AZIN2 splice variant facilitates endogenous cardiac regeneration. *Cardiovasc Res* **114**: 1642-1655.
14. Cho, H, Li, Y, Archacki, S, Wang, F, Yu, G, Chakrabarti, S, Guo, Y, Chen, Q, and Wang, QK (2020). Splice variants of lncRNA RNA ANRIL exert opposing effects on endothelial cell activities associated with coronary artery disease. *RNA Biol* **17**: 1391-1401.
15. Uchida, S, and Dimmeler, S (2015). Long noncoding RNAs in cardiovascular diseases. *Circ Res* **116**: 737-750.
16. Brannan, CI, Dees, EC, Ingram, RS, and Tilghman, SM (1990). The product of the H19 gene may function as an RNA. *Mol Cell Biol* **10**: 28-36.
17. Huang, P, Wang, L, Li, Q, Tian, X, Xu, J, Xu, J, Xiong, Y, Chen, G, Qian, H, Jin, C*, et al.* (2020). Atorvastatin enhances the therapeutic efficacy of mesenchymal stem cells-derived exosomes in acute myocardial infarction via up-regulating long non-coding RNA H19. *Cardiovasc Res* **116**: 353-367.

18. Lorenz, R, Bernhart, SH, Honer Zu Siederdissen, C, Tafer, H, Flamm, C, Stadler, PF, and Hofacker, IL (2011). ViennaRNA Package 2.0. *Algorithms Mol Biol* **6**: 26.
19. Martens, L, Ruhle, F, and Stoll, M (2017). LncRNA secondary structure in the cardiovascular system. *Noncoding RNA Res* **2**: 137-142.
20. Viereck, J, Buhrke, A, Foinquinos, A, Chatterjee, S, Kleeberger, JA, Xiao, K, Janssen-Peters, H, Batkai, S, Ramanujam, D, Kraft, T*, et al.* (2020). Targeting muscle-enriched long non-coding RNA H19 reverses pathological cardiac hypertrophy. *Eur Heart J* **41**: 3462-3474.
21. Baronti, L, Karlsson, H, Marusic, M, and Petzold, K (2018). A guide to large-scale RNA sample preparation. *Anal Bioanal Chem* **410**: 3239-3252.
22. Karbasiafshar, C, Sellke, FW, and Abid, MR (2021). Mesenchymal stem cell-derived extracellular vesicles in the failing heart: past, present, and future. *Am J Physiol Heart Circ Physiol* **320**: H1999-H2010.
23. Monguio-Tortajada, M, Prat-Vidal, C, Martinez-Falguera, D, Teis, A, Soler-Botija, C, Courageux, Y, Munizaga-Larroude, M, Moron-Font, M, Bayes-Genis, A, Borras, FE*, et al.* (2022). Acellular cardiac scaffolds enriched with MSC-derived extracellular vesicles limit ventricular remodelling and exert local and systemic immunomodulation in a myocardial infarction porcine model. *Theranostics* **12**: 4656-4670.
24. Watson, SA, Scigliano, M, Bardi, I, Ascione, R, Terracciano, CM, and Perbellini, F (2017). Preparation of viable adult ventricular myocardial slices from large and small mammals. *Nat Protoc* **12**: 2623-2639.
25. Marin-Sedeno, E, de Morentin, XM, Perez-Pomares, JM, Gomez-Cabrero, D, and Ruiz-Villalba, A (2021). Understanding the Adult Mammalian Heart at Single-Cell RNA-Seq Resolution. *Front Cell Dev Biol* **9**: 645276.
26. Anversa, P, Olivetti, G, Melissari, M, and Loud, AV (1980). Stereological measurement of cellular and subcellular hypertrophy and hyperplasia in the papillary muscle of adult rat. *J Mol Cell Cardiol* **12**: 781-795.
27. Khetan, J, Shahinuzzaman, M, Barua, S, and Barua, D (2019). Quantitative Analysis of the Correlation between Cell Size and Cellular Uptake of Particles. *Biophys J* **116**: 347-359.
28. Zhang, Y, Huang, W, Yuan, Y, Li, J, Wu, J, Yu, J, He, Y, Wei, Z, and Zhang, C (2020). Long non-coding RNA H19 promotes colorectal cancer metastasis via binding to hnRNPA2B1. *J Exp Clin Cancer Res* **39**: 141.
29. Lei, Y, Guo, W, Chen, B, Chen, L, Gong, J, and Li, W (2018). Tumorreleased lncRNA H19 promotes gefitinib resistance via packaging into exosomes in nonsmall cell lung cancer. *Oncol Rep* **40**: 3438-3446.
30. Mentkowski, KI, and Lang, JK (2019). Exosomes Engineered to Express a Cardiomyocyte Binding Peptide Demonstrate Improved Cardiac Retention in Vivo. *Sci Rep* **9**: 10041.

LIST OF FIGURE LEGENDS

Figure 1 – lncRNA H19 has 16 splice variants and their expression decrease through development. a) mouse H19 gene is located in the reverse strand of chromosome 7. Sixteen splice variants have been annotated. Mouse genome reference GRCm39:CM001000.3; **b)** Table with the splice variants detected by the 5 designed primer pairs; **c)** RT-qPCR analysis of different H19 splice variant sets present in hearts from embryo or adult mouse, showing downregulation of all the tested splice variants in adult hearts. *Error bars* are represented as Geometric Mean and Geometric SD; * p≤0,05; ***p≤0,001; ****p≤0,0001.

Figure 2 – Transfection of plasmid DNA encoding H19 leads to the transcription of different H19 splice variants that are then packaged and released in extracellular vesicles. a) Schematic representation of WJ-MSC transfection with pCMV6-H19 or pCMV6-Entry followed by extracellular vesicle isolation; **b)** RT-qPCR analysis of different H19 splice variants expressed by WJ-MSC 48h after transfection, demonstrating that all tested splice variants are expressed in the cells; **c-g)** EV-Entry and EV-H19 characterization demonstrating similar (c) size distribution, (d) particle concentration after isolation, (e) zeta potential, (f) protein concentration and (g) particles/ µg protein; **h)** RT-qPCR analysis of different H19 splice variants present in the EV isolated from transfected WJ-MSC, demonstrating that all tested splice variants are present in the EV albeit at different ratios than the ones found in the parental cells. *Error bars* are represented as Mean ± SD; * p≤0,05.

Figure 3 – Cardiomyocytes, fibroblasts and endothelial cells quickly uptake EVs and increase the expression of most of the H19 splice variants upon treatment with EV-H19. a) Representative confocal image depicting EV internalization by neonatal mouse cardiomyocytes. *Scale bar* is 20 µm; **b)** RT-qPCR analysis of different H19 splice variants expressed by cardiomyocytes after 4h incubation with EV-Entry or EV-H19; **c)** Representative confocal image depicting EV internalization by neonatal mouse cardiac fibroblasts. *Scale bar* is 20 µm; **d)** RT-qPCR analysis of different H19 splice variants expressed by fibroblasts after 4h incubation with EV-Entry or EV-H19; **e)** Representative confocal image depicting EV internalization by aortic endothelial cells. *Scale bar* is 20 µm; **f)** RT-qPCR analysis of different H19 splice variants expressed by endothelial cells after 4h incubation with EV-Entry or EV-H19; *Error bars* are represented as Mean ± SD; * p≤0,05; ** p≤0,01; ***p≤0,001.

Figure 4 – EV are internalized by cardiomyocytes and endothelial cells both throughout the cardiac slice. a) Representative confocal images of cardiac slices incubated for 24h with PKH67 labelled EV. *Scale bar* is 50 µm. *White arrows* indicate EV taken up by a cardiomyocyte (CM), *yellow arrows* indicate EV internalized by endothelial cells (EC) and *violet arrows* indicate EV internalized by other non-labelled cells (other). Imaged is zoomed in to allow the identification of EV foci in EC (top) and in cardiomyocytes (bottom); **b)** Sum of the EV *foci* that colocalizes with a cardiomyocyte (CM), with an endothelial cell (EC) or with none of the prior cells (other) quantified in three z-stacks of eight "z" for each independent cardiac slice (n), after 24h incubation, demonstrating EV internalization by CM, EC and other cells; *Error bars* are represented as Mean ± SD; ** $p \leq 0{,}01$.

a

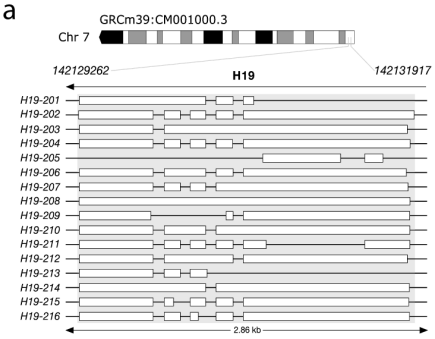

c

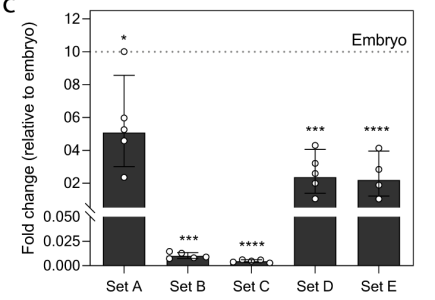

b

H19 Isoforms	Set A	Set B	Set C	Set D	Set E
201	X				
202		X	X		
203		X		X	X
204		X	X		
205					
206		X		X	X
207		X	X		
208	X	X			X
209		X			
210		X			X
211		X	X		
212		X		X	X
213			X		
214	X	X			X
215		X			
216		X	X		

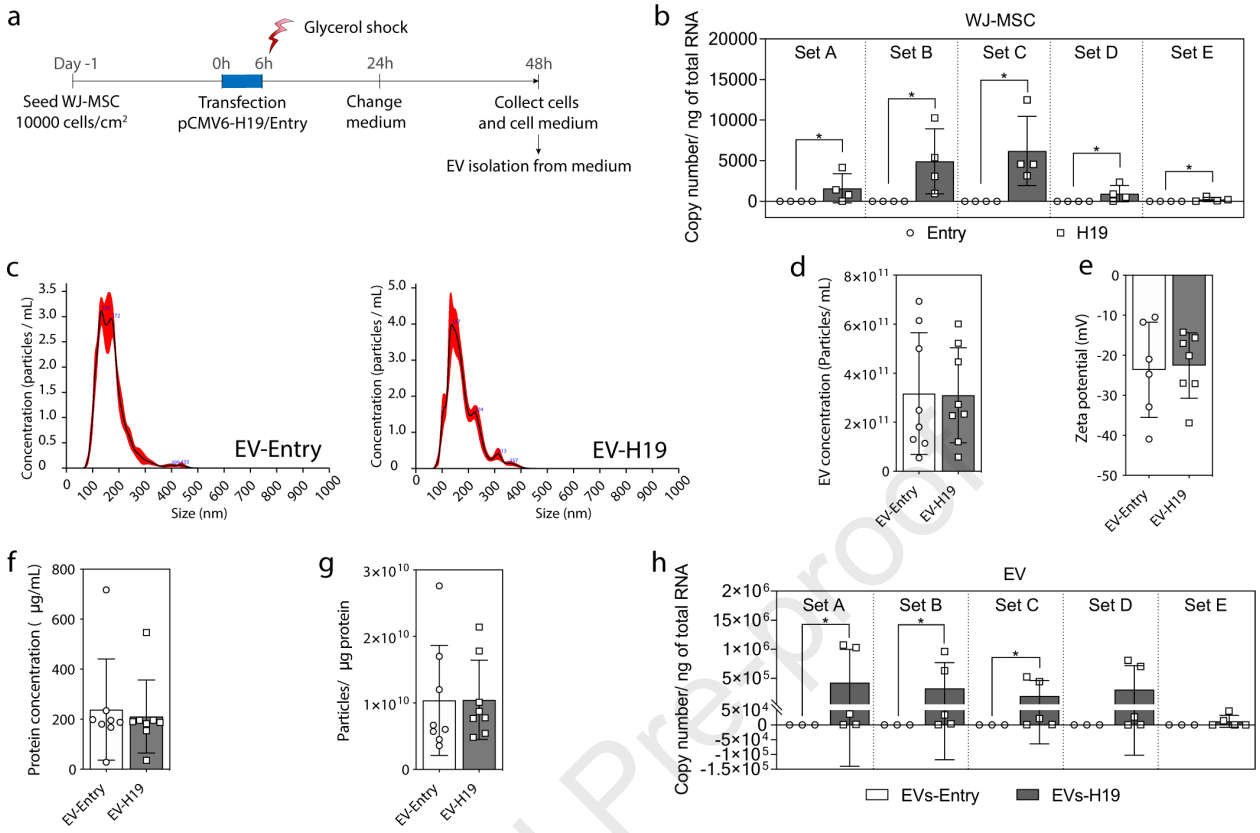

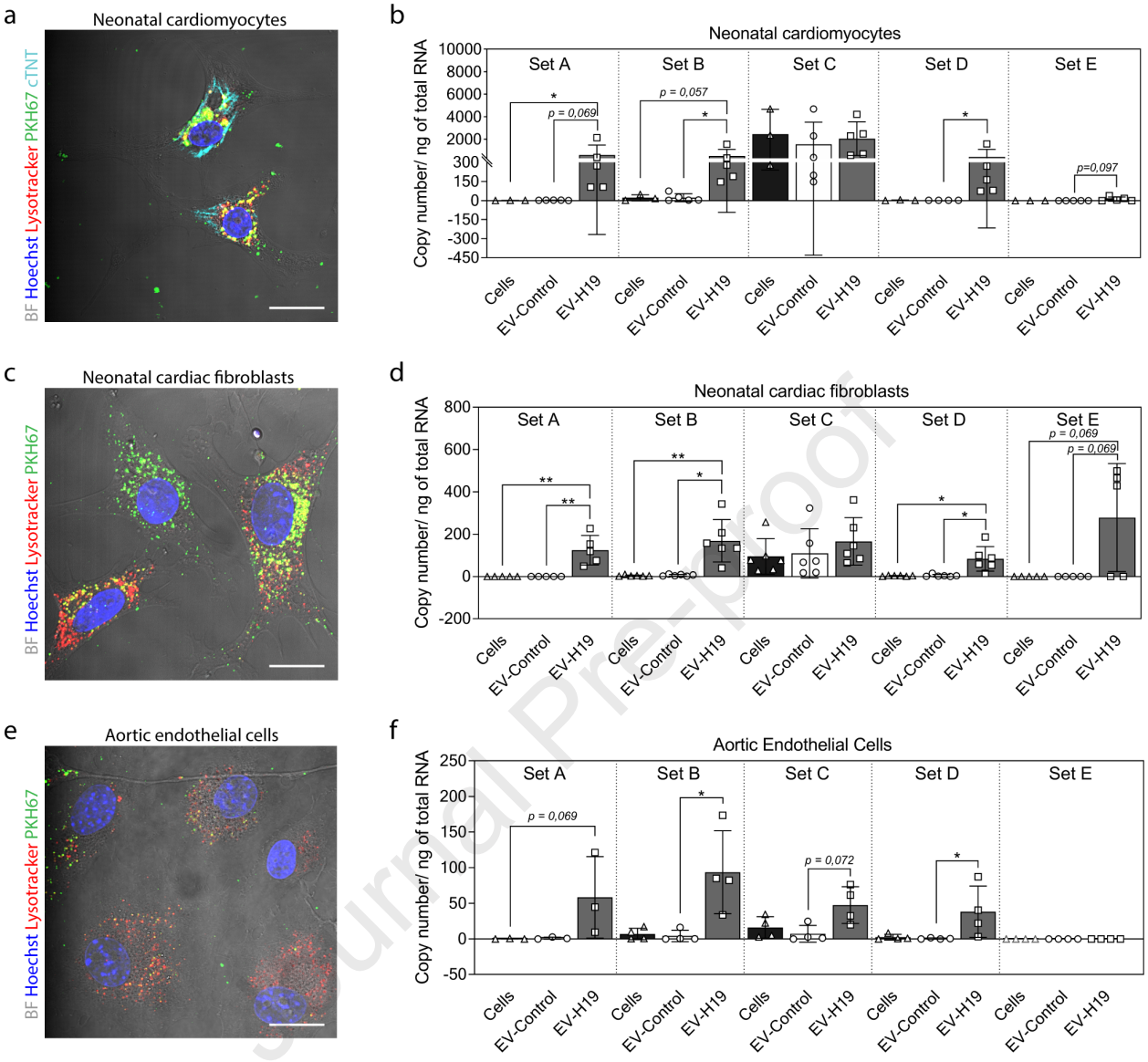
a
Neonatal cardiomyocytes
BF Hoechst Lysotracker PKH67 cTNT
b
Neonatal cardiomyocytes
Copy number/ ng of total RNA
Set A
Set B
Set C
Set D
Set E
p = 0,069
p = 0,057
p=0,097
Cells
EV-Control
EV-H19
c
Neonatal cardiac fibroblasts
BF Hoechst Lysotracker PKH67
d
Neonatal cardiac fibroblasts
Copy number/ ng of total RNA
p = 0,069
e
Aortic endothelial cells
BF Hoechst Lysotracker PKH67
f
Aortic Endothelial Cells
Copy number/ ng of total RNA
p = 0,069
p = 0,072

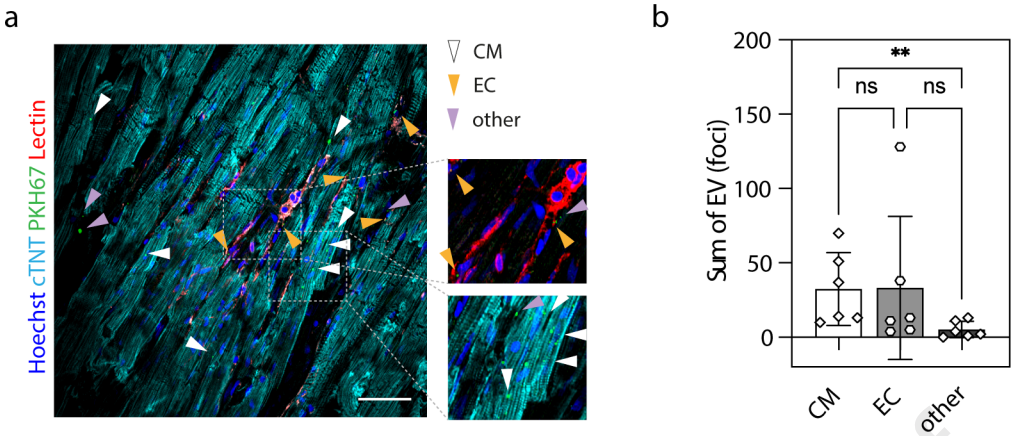

Vilaça and colleagues showed that extracellular vesicles secreted by Wharton-Jelly mesenchymal stromal/stem cells following overexpression of the long non-coding RNA H19 contain different H19 slice variants. These vesicles are internalized by cardiac cells, in cell cultures and rat living myocardial slices, transfecting the former with different H19 splice variants.